

Signature Intensity Derivative and its Application to Resident Space Object Typing

Tamara Payne and Anil Chaudhary

Applied Optimization Inc.

Stephen Gregory

Boeing LTS Inc.

James Brown

AFRL/RVBYB

Mark Nosek

AFRL/RYJW

ABSTRACT

A key feature of resident space object (RSO) photometric signatures is change in their brightness and color with time. It has been discovered that because of the illumination angle dependency of this temporal nature, time alone is insufficient to characterize the intrinsic nature of change in signature brightness. In this paper, we present a derivation of how the first derivative of the photometric intensity as a function of phase angle is related to the normalized reflectance spectra of the materials contained in the RSO signature. It is shown for the case of the geosynchronous orbit satellite and the results of a test case in this orbit regime are presented. We discuss the implications on existing characterization algorithms and its potential for the development of new algorithms that process the photometric signatures. Finally, we discuss the insights obtained by this analysis on photometric data collection techniques.

1. INTRODUCTION

There is great interest in being able de-convolve resident space object (RSO) photometric signatures in a way that it creates a better understanding about the operational status and behavior of the RSO. The methods designed for such signature de-convolution fall in the realm of inverse problems. They are usually ill-posed from a mathematical standpoint and its pertinence is that the uniqueness of the solution is difficult to prove. This commonly occurs for two reasons. First is a case when two or more unknown parameters of interest only appear as product in the signature, e.g. albedo and area. Because the two parameters cannot be separated from within the product, the available data are posed in terms of ratios, which can allow cancellation of the parameter that does not change, e.g. area, and only the normalized or relative values of the parameters can be solved. Second is when the number of unknowns exceeds the number of independent equations available. This results in a rectangular system of equations, which are solved using a technique such as singular value decomposition. This provides a solution that is deemed a best fit. Because the uniqueness of solution is difficult to prove mathematically, the algorithms that endure the test of time are commonly based on physical arguments that represent fundamental truths. Then, even if uniqueness cannot be proven, it is feasible to ascertain the validity of such a solution. The signature derivative technique is one such method that is based on simple, intuitive, and physical arguments for separation of reflectance spectra from RSO signatures. It makes use of our knowledge that solar panels track the sun, and creates additional independent conditions that are pivotal to the separation.

A RSO photometric signature contains contributions from its solar panels and body surfaces. The proportion of contribution from each surface depends on its individual reflectance spectrum, the direction of illumination, and the projected view of the RSO with respect to the sensor. From these three, the latter two are known for many objects. The reflectance spectra, however, are generally not known well. This is either because the RSO materials themselves are not known or the data is available only for the beginning-of-life condition for the known materials. It is well known that RSO materials age in space and as a consequence their spectral reflectance changes. Within the visible portion of the electro-magnetic spectrum, these changes have been observed to be a function of wavelength. It is also observed that the extent of aging effect varies from one RSO to another, even if both belong to the same family of spacecraft and are of comparable age. The lack of knowledge of the RSO's true material spectral properties results in an ill-posed mathematical problem, where the number of unknowns exceeds the number of independent equations and this ill-posing persists irrespective of the spectral resolution of the signature. Thus, as

Report Documentation Page				Form Approved OMB No. 0704-0188	
Public reporting burden for the collection of information is estimated to average 1 hour per response, including the time for reviewing instructions, searching existing data sources, gathering and maintaining the data needed, and completing and reviewing the collection of information. Send comments regarding this burden estimate or any other aspect of this collection of information, including suggestions for reducing this burden, to Washington Headquarters Services, Directorate for Information Operations and Reports, 1215 Jefferson Davis Highway, Suite 1204, Arlington VA 22202-4302. Respondents should be aware that notwithstanding any other provision of law, no person shall be subject to a penalty for failing to comply with a collection of information if it does not display a currently valid OMB control number.					
1. REPORT DATE SEP 2009		2. REPORT TYPE		3. DATES COVERED 00-00-2009 to 00-00-2009	
4. TITLE AND SUBTITLE Signature Intensity Derivative and its Application to Resident Space Object Typing				5a. CONTRACT NUMBER	
				5b. GRANT NUMBER	
				5c. PROGRAM ELEMENT NUMBER	
6. AUTHOR(S)				5d. PROJECT NUMBER	
				5e. TASK NUMBER	
				5f. WORK UNIT NUMBER	
7. PERFORMING ORGANIZATION NAME(S) AND ADDRESS(ES) Air Force Research Laboratory, AFRL/RVBYB, Hanscom AFB, MA, 01731				8. PERFORMING ORGANIZATION REPORT NUMBER	
9. SPONSORING/MONITORING AGENCY NAME(S) AND ADDRESS(ES)				10. SPONSOR/MONITOR'S ACRONYM(S)	
				11. SPONSOR/MONITOR'S REPORT NUMBER(S)	
12. DISTRIBUTION/AVAILABILITY STATEMENT Approved for public release; distribution unlimited					
13. SUPPLEMENTARY NOTES 2009 Advanced Maui Optical and Space Surveillance Technologies Conference, 1-4 Sep, Maui, HI.					
14. ABSTRACT A key feature of resident space object (RSO) photometric signatures is change in their brightness and color with time. It has been discovered that because of the illumination angle dependency of this temporal nature, time alone is insufficient to characterize the intrinsic nature of change in signature brightness. In this paper, we present a derivation of how the first derivative of the photometric intensity as a function of phase angle is related to the normalized reflectance spectra of the materials contained in the RSO signature. It is shown for the case of the geosynchronous orbit satellite and the results of a test case in this orbit regime are presented. We discuss the implications on existing characterization algorithms and its potential for the development of new algorithms that process the photometric signatures. Finally, we discuss the insights obtained by this analysis on photometric data collection techniques.					
15. SUBJECT TERMS					
16. SECURITY CLASSIFICATION OF:			17. LIMITATION OF ABSTRACT	18. NUMBER OF PAGES	19a. NAME OF RESPONSIBLE PERSON
a. REPORT unclassified	b. ABSTRACT unclassified	c. THIS PAGE unclassified			

regards to attaining uniqueness of inverse solution, a hyperspectral signature offers no advantage over signatures obtained using filter photometry, such as Johnson B, V, R and I.

Now consider if a certain projected view of a RSO was to comprise a single material, the spectral shape of its signature would be directly proportional to the reflectance spectrum of that material. This is called a purity condition because it allows extraction of a normalized reflectance spectrum. Since it is extracted from the RSO signature, it intrinsically includes the effect of aging. The calculation of an absolute reflectance spectrum also requires knowledge of the RSO geometry and its orientation with respect to the sun and the sensor. It is, however, notoriously difficult to obtain signatures that only contain a single material. Theoretically, it is possible for RSOs in the low-earth orbit. It is not practical for deep-space RSOs. Furthermore, for unknown RSOs, its geometric configuration and orientation in space are not known either. This results in an inverse problem that is ill-posed no matter how it is formulated and makes characterization of unknown RSOs very challenging.

Unmixing of the material contributions from the RSO signature is one approach to the inverse solution. It uses a known and finite set of normalized material spectra, which are mostly for the beginning-of-life condition. The algorithm finds a combination of materials from this set and the fractional abundances thereof that can best represent the RSO signature. There are many useful results reported with unmixing, but questions remain. This is because there is no certainty that the set of material spectra used in the unmixing are both complete and accurate for the RSO in question. Thus, in spite of seemingly useful results, it is difficult to ascertain a probability of false alarm, which is essential in order to lend credence to the RSO characterization results.

Traditionally, RSO characterization is done using panchromatic photometry taken in the visible portion of the spectrum. These data comprise discrete values of signature brightness usually reported in visual magnitude. The brightness values can then be tabulated as a function of the solar phase angle, which is the sun-RSO-observer angle. Collection of such data over the years provides a probability distribution function for the RSO brightness as a function of the phase angle. A newly observed visual magnitude can then be compared with the historical data in order to ascertain if it is normal or anomalous. Being panchromatic data, this approach has limitations, particularly in tasks such as the resolution of mis-tagged RSOs.

Even though there are the above mentioned challenges, a signature from a spatially non-resolved image is and will always be a primary window for information for understanding the status of RSOs, particularly the uncooperative RSOs and deep space RSOs. It is valuable to attain purity conditions so that reflectance spectrum for an aged material, devoid of contributions from other unknown and/or aged materials, can be extracted from the signature. These material spectra can then be used as input for unmixing calculations that divulge further insight. The material spectra are invaluable in order to enhance the traditional panchromatic RSO characterization that uses brightness values at isolated, discrete values of phase angle. The signature derivative technique is a way to overcome the barriers to attaining the purity conditions. The rationale for this method is based on the analytical solution for a flat plate signature. It is used to develop a set of hypotheses and a mode of usage for backward tracing. Such a technique is described in this paper and includes the derivation of the signature derivatives and its testing with the photometric signature data collected on a RSO in geosynchronous orbit (GEO).

2. SIGNATURE INTENSITY GRADIENT DERIVATION

Consider a flat plate such as the one shown in Fig. 1 that is illuminated by the sun and a sensor that collects a photometric signature of its reflected sunlight. The flat plate is meant to represent a single planar facet with the generalization that a RSO can be represented as a faceted geometry in which one or more components articulate in performing their function. For example, the solar panels track the sun, antennae may point to ground-based receivers, etc. The sun-facet-sensor angle is γ , which is the solar phase angle. The angle of illumination (sun angle) is β . The angle of reflection is equal to $\gamma - \beta$. The range normalized signature for a planar facet is given by a product of the albedo, area and cosines of angles β and $(\gamma - \beta)$, where we have generalized the term albedo to refer to the fraction of reflected (both diffuse and specular) light to incident light. Then the closed-form expression for the range-normalized signature, I , can be written as:

$$I = L \cos \beta \cos(\gamma - \beta) = \frac{L}{2} (\cos \gamma + \cos(\gamma - 2\beta))$$

where L is the albedo-area product. If the RSO geometry was to comprise a total of n planar-facets, its range normalized signature is given as follows where the subscript, f, is a facet number:

$$I = \sum_{f=1}^n \frac{L_f}{2} (\cos \gamma + \cos(\gamma - 2\beta_f))$$

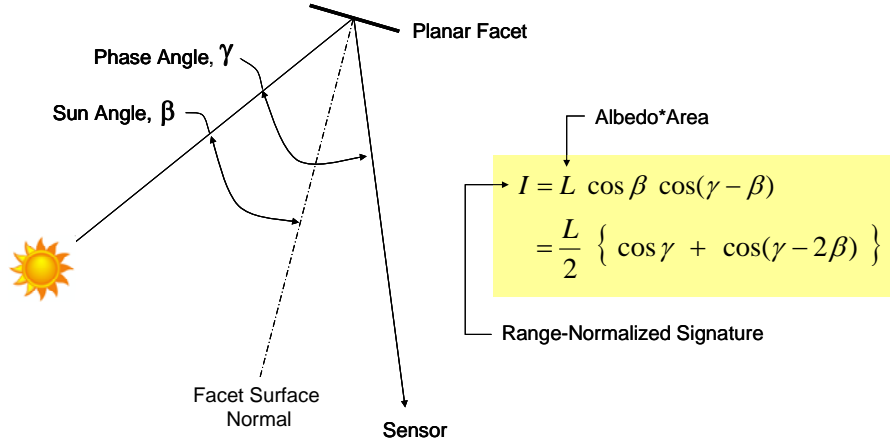


Fig. 1: Planar facet reflection geometry

This expression simplifies under certain conditions when the angles β and γ assume the values shown in Table 1. Specifically, for any surface that glints, the phase angle bisector condition is satisfied. This occurs for any facet when β is one-half of the solar phase angle γ .

Table 1: Simplified closed form expression for the range-normalized signature

RSO Surface	Value of Angle	Range Normalized Signature
Glinting Facets	$\beta = \gamma / 2$	$L(\cos \gamma + 1)/2$
Solar Panel	$\beta = 0$	$L \cos \gamma$

Now consider a set of photometric signatures from a GEO. Fig. 2 shows an example of such a set. They are denoted as G1, G2, G3, etc. These signatures were observed from the same ground-based site. The GEO has two solar panels and a complex body. Fig. 2 shows how the signature brightness changes as a function of the longitudinal component of the phase angle. At a phase angle close to zero, the signature brightens significantly. This is when the specular glint condition for the solar panels is reached. It should ideally occur when phase angle equals zero. It, however, has a small offset. This is because GEO satellites are frequently operated with their solar panels not exactly pointed toward the sun as a means to react to the orbital perturbation caused by the solar radiation pressure. As the absolute value of the phase angle increases, the signature becomes dimmer.

Our first hypothesis contains three parts, which are the implications that are based on the analytical expression for the range-normalized signature.

- *Hypothesis 1a:* The undulations in the signature represent the effects of specular glints from small features and self-occlusion of the RSO body. As a result, they are present even in the case of stable RSOs. For example, the GEO in Fig. 2 has antennae that have a complex interaction with the incident sunlight, which is potentially manifested as undulations in brightness.

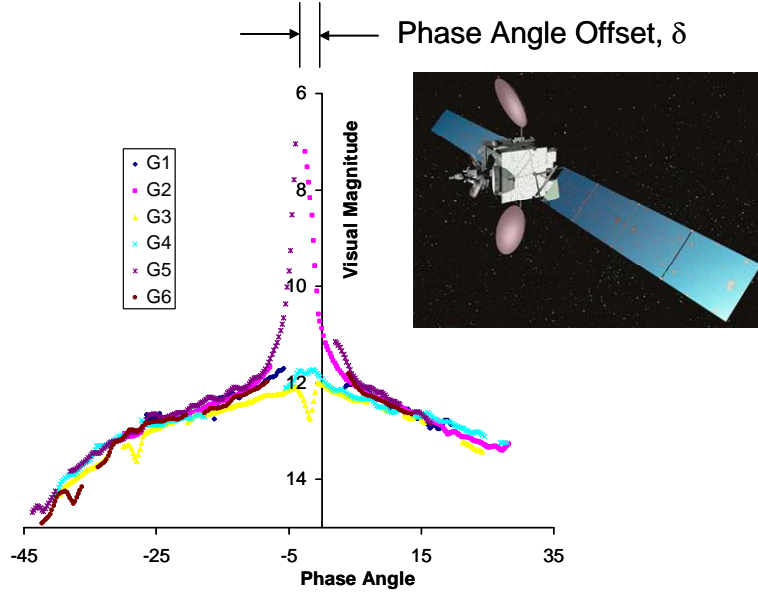


Fig. 2: Six B-band signatures for a Geosynchronous Satellite

- *Hypothesis 1b:* The contribution of the solar panels is symmetric with respect to the phase angle since they track the sun. The signature, however, is asymmetric with respect to the phase angle. Therefore, the signature asymmetry is a function of asymmetry in the body geometry. For example, for the GEO satellite in Fig. 2, the positive phase angle may be a situation when the body is illuminated from, say the right side. Then, the negative phase angle would be when the body is illuminated from the left side. Thus the signature asymmetry represents how the body signature is different when it is illuminated differently. This may be considered a distinguishing feature between satellites.
- *Hypothesis 1c:* The sum-of-cosines form of the analytical solution provides rationale for use of a discrete cosine transform for representation of the time-frequency behavior in the signature, where ‘time’ is represented by the cosine of the phase angle. This is natural because the analytical expression is ‘linear’ in the cosine of the phase angle under multiple conditions of practical interest.

The next hypothesis has two parts that address the solar panel contribution to the signature and its implications based on the cosine terms in the analytical expression.

- *Hypothesis 2a:* The solar panel offset, δ , is a feature of GEO signatures since its value is set by the satellite operator in order to manage the solar radiation pressure and the resulting torque. For the solar panels, angle β equals $\delta/2$ and its signature at any phase angle is then given by:

$$I = \left(L \cos \frac{\delta}{2} \right) \cos \left(\gamma - \frac{\delta}{2} \right).$$

- *Hypothesis 2b:* The solar panel signature is a linear function of $\cos(\gamma - \delta/2)$, which is an even function. Or, the contribution of the solar panel to the total signature is symmetric about the specular peak. Thus, the signature can be folded about the specular peak and plotted against $\cos(\gamma - \delta/2)$ instead of the phase angle γ . Fig. 3 shows the same signatures in Fig. 2 upon folding and plotting against $\cos(\gamma - \delta/2)$.

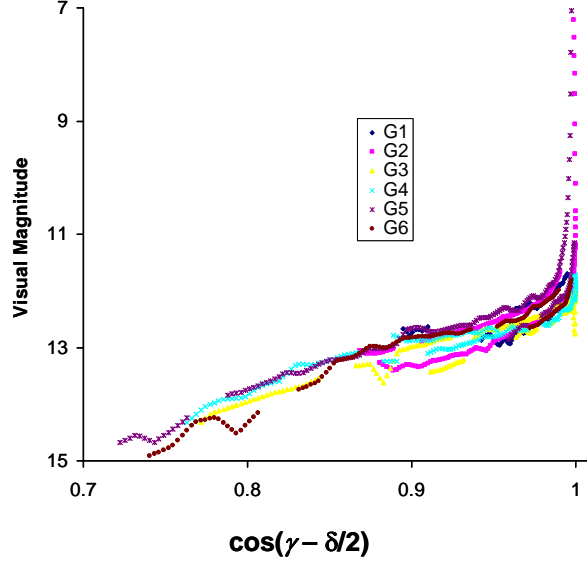


Fig. 3: Folded B signatures of Galaxy 10R as a function of $\cos(\gamma - \delta/2)$

The third hypothesis comprises two implications based on the specular glint condition and is useful for extracting the normalized material spectra of the solar panel and the body.

- *Hypothesis 3a:* Consider signature data that contains a solar panel specular peak. In the neighborhood of the peak, the signature undergoes rapid change. Such a change in the signature allows extraction of material reflectance spectra for both the solar panel and the body. Assume the specular peak is defined as the region where $\cos(\gamma - \delta/2)$ is > 0.98 (see Fig. 2 and Fig. 3). The analytical expression for the total differential of the range-normalized signature is given by:

$$dI = \left\{ \sum_{f=1}^n \frac{L_f}{2} (-\sin\gamma + \sin(\gamma - 2\beta_f)) + \sum_{f=1}^n \frac{1}{2} \frac{dL_f}{d\gamma} (\cos\gamma + \cos(\gamma - 2\beta_f)) \right\} d\gamma$$

From geometrical considerations, we know the solar panel contribution to signature increases as the phase angle approaches the specular peak. Once the peak is past, the solar panel contribution decreases. Thus the rate of change of solar panel signature is positive as the phase angle approaches the specular peak and it is negative after the peak is past. In other words, the rate of change of solar panel signature is an odd function of the phase angle. For the solar panel facet, recall that $\gamma - 2\beta = 0$. Therefore, in this case we can rewrite the range-normalized signature as follows:

$$dI_f = \left\{ \frac{L_f}{2} (-\sin\gamma) + \frac{1}{2} \frac{dL_f}{d\gamma} (\cos\gamma + 1) \right\} d\gamma$$

This is an odd function of the phase angle. This can be confirmed by considering the signs of each term when the phase angle crosses zero. For example, let the phase angle equal a small value, ε , where ε is greater than zero at the start. Upon crossing the specular peak, the value of ε becomes negative. Then, the expression can be written as follows:

$$dI_f = \left\{ \frac{L_f}{2} (-\sin\varepsilon) + \frac{1}{2} \frac{dL_f}{d\gamma} (\cos\varepsilon + 1) \right\} d\gamma$$

When the specular peak is incipient, $\varepsilon > 0$, the first term is negative, and since the rate of change of solar panel albedo-area product is positive, the second term is positive. Once the specular peak is past, $\varepsilon < 0$, so now the first term is positive, and since the specular peak is past, the rate of change of solar panel albedo-area product is negative and thus the second term is negative. Therefore in this latter case, both terms switch signs upon zero crossing and by definition, dI_f is an odd function of γ .

Assuming that the specular peak is narrow, the rate of change of body albedo-area product during the time of said peak may be considered to be constant. In other words, the function that describes the rate of

change of the body albedo-area product is an even function of the phase angle. Also since the specular peak is narrow, the value of β_f is constant in the limit and so the sign of dI_f does not change upon crossing the solar panel specular peak, i.e., body contribution is independent of the solar panel. Thus dI_f is an even function of γ . For a body facet, one may compute its rate of change about $\gamma = \delta/2$ as follows:

$$dI_f = \left\{ \frac{L_f}{2} \left(-\sin \frac{\delta}{2} + \sin \left(\frac{\delta}{2} - 2\beta_f \right) \right) + \frac{1}{2} \frac{dL_f}{d\gamma} \left(\cos \frac{\delta}{2} + \cos \left(\frac{\delta}{2} - 2\beta_f \right) \right) \right\} d\gamma$$

It is now instructive to note that the sum of the above total differential just before the specular peak and just after the specular peak is equal to twice the rate of change of signature due to body facets. This is because the contribution of the solar panel cancels out (recall that it is an odd function). Therefore, this sum would yield the body material reflectance spectrum. Conversely, consider that the difference between the total differential of the signature before and after the specular peak equals twice the rate of change of signature due to the solar panel. This is because the body contribution cancels out since it is an even function. Therefore, this difference would yield the solar panel material reflectance spectrum.

This approach, which uses simple, physical arguments about the specular peak, circumvents a fundamental issue in attaining purity conditions, which are essential for separation of material reflectance spectra.

- *Hypothesis 3b:* We now extend the logic of Hypothesis 3a to the case of a specular glint that occurs when the phase angle bisector condition is met. This does not require the phase angle to be close to zero as in case of the solar panel glint, as in the case considered in 3a. This is a valid condition since glints can also originate from body facets.

Let the phase angle bisector condition be reached when the phase angle equals γ_0 . So under conditions near the glint, the phase angle is $\gamma = \gamma_0 + \varepsilon$, where ε is a small value. Then, the total differential for the range-normalized signature contribution from a glinting facet is given by:

$$dI_f = \left\{ \frac{L_f}{2} \left(-\sin(\gamma_0 + \varepsilon) \right) + \frac{1}{2} \frac{dL_f}{d\gamma} \left(\cos(\gamma_0 + \varepsilon) + 1 \right) \right\} d\varepsilon$$

Expanding the trigonometric terms and rearranging them suitably as terms that comprise an odd function with respect to γ_0 and the terms that comprise an even function, the following expression is obtained:

$$dI_f = \left\{ \frac{\cos \gamma_0 L_f}{2} \left(-\sin \varepsilon \right) + \frac{1}{2} \cos \gamma_0 \frac{dL_f}{d\gamma} \left(\cos \varepsilon + 1 \right) \right\} d\varepsilon - \left\{ \frac{\sin \gamma_0 L_f}{2} \cos \varepsilon + \frac{1}{2} \sin \gamma_0 \frac{dL_f}{d\gamma} \sin \varepsilon \right\} d\varepsilon$$

The first brace contains the odd function terms and the second contains the even function terms. As for the non-glinting facets, they are considered in the same way as in Hypothesis 3a. In other words, the rate of change of signature for the non-glinting facets is considered to be constant within the glinting region and it results in an even function with respect to γ_0 .

The difference between the total differential of the signature before and after the glint equals twice the rate of change of signature due to the odd terms in the contribution by the glinting facet. This is because the contribution by its even terms cancels out and so does the contribution by other, non-glinting facets (also even). Therefore, this difference in the total differentials would yield the reflectance spectrum for the glinting facet.

- *Hypothesis 4:* This hypothesis allows the separation of the body spectrum as a function of phase angle. If the body is asymmetric, then the body spectrum thus calculated is the mean spectrum of all the body materials. This is shown by considering that the solar panel signature is symmetric with respect to the phase angle value equal to δ (the solar panel offset angle). In other words, the solar panel contribution to the signature is equal for a negative phase angle γ_1 and a positive phase angle γ_2 if $\delta - \gamma_1 = \gamma_2 - \delta$. Now define a difference between the signatures at γ_2 and γ_1 , such that:

$$\Delta I = I(\gamma_2) - I(\gamma_1)$$

The contribution by the solar panel cancels when this difference is computed by the same symmetry arguments as before. Therefore, the quantity ΔI is the difference in the body contribution at γ_2 and γ_1 , respectively. Furthermore, the value of ΔI equals zero when γ_2 and γ_1 equal $\delta+\varepsilon$ and $\delta-\varepsilon$, respectively, when ε tends to zero.

Now using Hypothesis 3a, the solar panel and body material spectra are solved for in the interval $[\delta+\varepsilon$ to $\delta-\varepsilon]$. This allows the calculation of the albedo-area product for the body in the interval $[\delta+\varepsilon$ to $\delta-\varepsilon]$. Let us denote it as $I_{Body}(\delta)$. Then this is the initial condition needed in order to determine the mean value of the body spectrum, where mean is defined as the average of the body spectrum at γ_2 and γ_1 . This mean spectrum is given by:

$$I_{Body}^{Mean}(\gamma_2) = I_{Body}(\delta) + \Delta I / 2$$

3. CASE STUDY FOR A GEOSYNCHRONOUS SATELLITE

To test the hypotheses used to derive the signature gradients in Section 2, we turn our attention to a significant collection of photometric data on the RSO in GEO orbit, namely AMC 2. We assert that if these hypotheses are valid, then the solar panel and body material normalized spectra that can be calculated from the derivatives should be an invariant under the data collection conditions. Stated in another way, although the phase angle conditions under which the signature data is collected vary, the solar panel and body material spectra do not. Therefore, if the signature gradient processing technique for analytical unmixing is valid, it should yield similar values for the normalized spectrum of the solar panels and the body.

Even though there is more than a trivial amount of data on this RSO, there are challenges in the analysis of real data. These challenges occur due to pockets of low SNR, gaps in the data, non-uniform sampling rate, etc. that cannot be avoided in most observational data. Therefore, although this case is adequate for testing, it is not ideal. Its adequacy lies in that observations were collected at time periods which provide useful bounds on the extrema of phase angle experienced by GEO RSOs. The data were taken near the times of the Vernal Equinox, the Winter Solstice, and the Summer Solstice. Fig. 4 illustrates these extrema that bound the illumination conditions for GEOs.

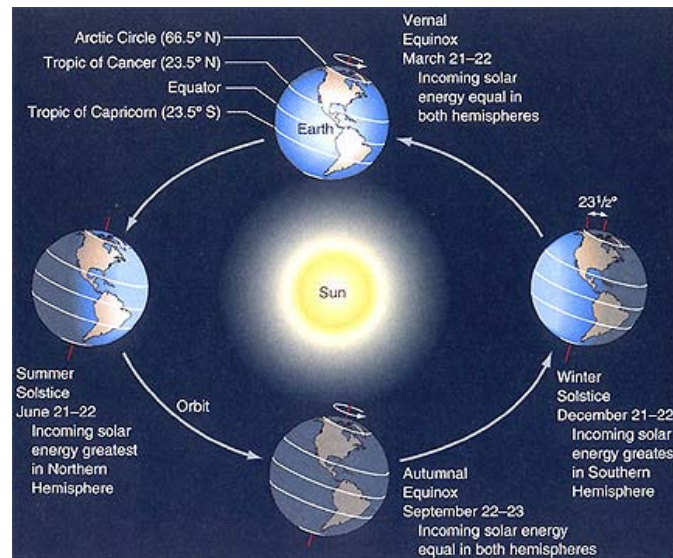


Fig. 4: Earth and Sun positions that bound the illumination conditions for GEOs

Figs. 5, 6, and 7 show the signatures taken at these three times using the same scales. It can be seen from the notations in each figure that the data were taken in different years with different combinations of the broad-band Johnson filters (B, V, R, and I). Furthermore, these data were taken using two different telescope/sensor systems. They are intercomparable since they were reduced using the same astronomical calibration techniques to remove errors induced by optics and the atmosphere via well-measured calibration standard stars.

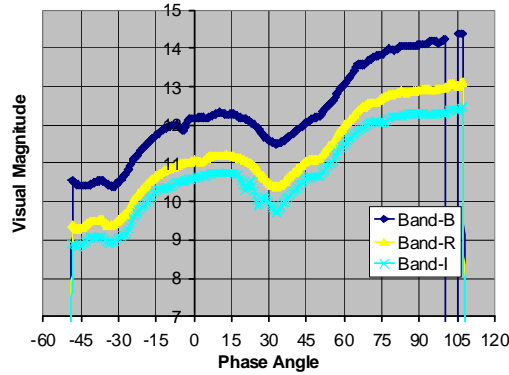


Fig. 5: Photometric signatures of AMC 2 at winter solstice (15 Jan 2008) taken with Kirtland Raven telescope

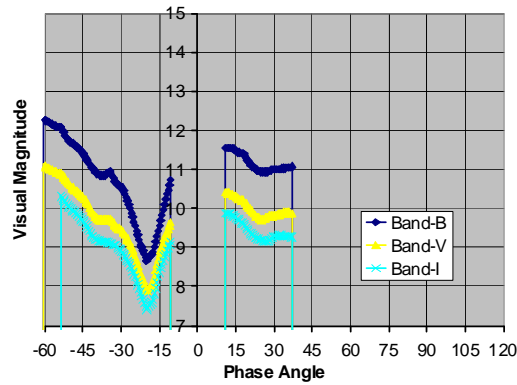


Fig. 6: Photometric signatures of AMC 2 at vernal equinox (18 Mar 2008) taken with Kirtland Raven telescope

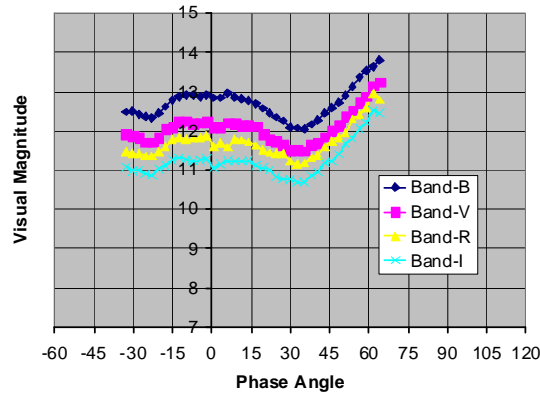


Fig. 7: Photometric signatures of AMC 2 at summer solstice (8 Jun 2005) with 40-inch Ritchey-Chretien telescope at Naval Observatory, Flagstaff Station.

An initial examination of Figs. 5 – 7 shows that these signatures exhibit various features in brightness, specular peaks, and orientation of the curves. However, closer examination yields there are some similarities, namely:

- The signature has a double-peak catenary-like shape. One peak is brighter than the other. The peaks are brighter at the equinox,
- At the solstices, a distinct peak occurs at phase angle $+33^\circ$. At the equinox, a distinct peak occurs at phase angle equal to -20° , and
- At the solstices, the positive phase angle peaks are broader. Their full-width-half-maximum (i.e., FWHM) is 15° . At the equinox, the negative phase angle peak is narrow and its FWHM is 8° .

Now, let us calculate the normalized solar panel and body material spectra using the signature derivatives. This idealizes a RSO as a set of planar facets for which both the geometry and orientation are not known a priori. Let I be the range and phase angle normalized photometric signature in some wavelength band. Then the first partial derivative of I with respect to the cosine of the phase angle provides the material spectra for the solar panel and body. We have for the signature, I , normalized by $\cos \gamma$:

$$\frac{I}{\cos \gamma} = L_{SolarPanels} + \sum \frac{L_{Body}}{2} + \sum \frac{L_{Body}}{2} \frac{\cos(\gamma - 2\beta)}{\cos \gamma}$$

Note that, in the above expression, the subscript f is dropped for the sake of brevity. It is implicit that the summation is over all body facets. If we take the first derivative of this expression with respect to $\cos \gamma$, and consider two cases:

- Case 1: For phase angles away from the specular peaks, the derivative is proportional to the body terms:

$$\frac{d}{d \cos \gamma} \left(\frac{I}{\cos \gamma} \right) = \sum \frac{L_{Body}}{2} \left[\frac{d}{d \cos \gamma} \left(\frac{\cos(\gamma - 2\beta)}{\cos \gamma} \right) \right]$$

- Case 2: For phase angles close to a specular peak, the derivative is proportional to the solar panel terms. This assumes that the body contribution remains unchanged as per Hypothesis 3a.

$$\frac{d}{d \cos \gamma} \left(\frac{I}{\cos \gamma} \right) = \frac{d}{d \cos \gamma} (L_{SolarPanels})$$

The derivatives of the signature data in Figure 5 (winter solstice) were calculated using the two equations directly above. For the winter solstice condition, the body material spectrum was calculated at phase angles greater than 45° . The solar panel material spectrum was calculated at phase angles from -30° to -20° . For the signatures in Fig. 6, i.e. the vernal equinox condition (sharp specular peak), the solar panel and body spectra were calculated using the equations in Hypothesis 3a. The signature data in Fig. 7 (summer solstice) was noisier and more difficult to achieve satisfactory results. Derivatives both close to the specular peak and at high phase angles ($56^\circ - 64^\circ$) were computed. The results are tabulated in Table 2. These values represent the material spectra of the solar panels and the body, where the spectral resolution is from the filter bands in B, V, R, and I at 440 nm, 550 nm, 700 nm, and 880 nm respectively, and the spectral values are normalized to the B band.

Table 2: Normalized material spectra extracted from 3 sets of signature data

Observation	B band	V band	R band	I band
<i>Solar Panel</i>				
Winter solstice	1.0	-	0.79	0.60
Vernal equinox	1.0	-	0.70	0.60
Summer solstice	1.0	0.81	0.70	0.56
<i>Body</i>				
Winter solstice	1.0	-	1.0	0.80
Vernal equinox	1.0	-	1.0	0.80
Summer solstice	1.0	0.87	1.04	0.76

It is encouraging to note that the solar panel and body spectra are consistent between observations. This was, however, done with human oversight, which keeps open the question of bias. Nonetheless, the calculations performed are quite mundane and can be repeated easily for any number of observations by a third party. This can build confidence in the reported values. Although this is only one case, this non-ideal example lends credence to our usage of the signature gradient derivatives to obtain material spectra.

4. CONCLUSIONS

We have derived from the closed-form of the range-normalized signature, expressions for the signature gradients that yield material spectra of the solar panels and the body based upon symmetry arguments. Additionally, we have shown a test case using these derivatives that yields acceptably consistent values for the solar panels and the body for a RSO in GEO orbit. This has important implications in the calculation of material abundances using any temporal unmixing algorithm. This is because the unmixing algorithms begin with a database of material spectra as input. The signature is processed to isolate the spectra that provide a best fit to the signature. A common criticism of the results is non-uniqueness. This analytical unmixing technique is a simple way to generate spectra for materials in situ. It also provides a pairing of materials that occur together, which could help resolve mis-identifications and aid in the separation of RSO shape and mechanics. In the general case of an RSO, consider that it can be observed over a period of time by different sensors, both ground and space-based. When a specular glint is observed, the material reflectance spectrum can be extracted. Since a glint can be observed repeatedly, the reflectance spectrum can be independently verified by multiple observers and over multiple observations. The collection of all reflectance spectra for this RSO can then become a part of the known information about its signature and how it appears under different phase angle conditions. The phase angle dependence of its signature can then be utilized to separate out the spectrum on a material that did not glint. This can then be compared with known spectra to ascertain materials composition or, at the very least, narrow down the number of possible materials. If the same material spectrum was determined and compared with its older values, it provides information on how the material spectrum is changing, which in turn provides clues on the aging for the RSO. The information obtained from analytical unmixing can thus be used as input for additional forms of analyses.

Any observational data is susceptible to error due to a variety of reasons. Thus there is a limit on the trust that may be placed on the information extracted from a single observation. However, if a similar result was obtained in an independent observation, then the probability of false alarm reduces. This reduction continues with more and more independent determinations. Furthermore, the calculations in Hypotheses 3a and 3b can be used repeatedly on data collected by different sensors to extract material reflectance spectra for the glinting facets. For example, glints from various body surfaces may be observed by a space-based sensor and then processed to extract the material spectrum for that material. Additional testing of this approach is being pursued using other types of data, namely visible and infrared spectral data of various spectral resolutions on RSOs in different orbital regimes.

5. ACKNOWLEDGMENTS

We express our gratitude to the Dr. Fred Vrba and the U. S. Naval Observatory, Flagstaff Station for their support and contribution to the data collection campaign that resulted in the signature in Figure 7. Additionally we are grateful to Mr. Paul Kervin (AFRL) and the HANDS program for the telescope time allocated to the collection of the signatures shown in Figures 2, 5, and 6.